GEOPHYSICAL RESEARCH LETTERS VOL. 40, 66–71, doi:10.1029/2012GL054116, 2013

Simultaneous partitioning of silicon and oxygen into the Earth's core during early Earth differentiation

Kyusei Tsuno,[1,2] Daniel J. Frost,[1] and David C. Rubie[1]

Received 5 October 2012; revised 19 November 2012; accepted 26 November 2012; published 16 January 2013.

[1] Silicon and oxygen are potential light elements in the Earth's core and may be involved in metal-silicate reactions at the present day core-mantle boundary. We have performed multianvil experiments at 25 GPa and 2770–3080 K to understand the simultaneous partitioning of these elements between liquid iron–rich metal and silicate melt. The presence of O in liquid Fe at high temperatures influences the partitioning of Si, causing more Si to partition into the metal than would be expected based on lower temperature measurements. Although Si and O are mutually exclusive in Fe metal at <3000 K, the level at which both element concentrations are similar in the liquid metal rises above 1 wt % at >3000 K. We have developed a thermodynamic model based on these experiments that accounts for the interaction between O and Si in the liquid metal. Comparison between this model and the previous results of diamond-anvil cell experiments up to 71 GPa indicates very little pressure dependence but a strong temperature dependence for O and Si partitioning. Our model predicts that subequal concentrations of Si and O, sufficient to explain the outer core density deficit, would have partitioned into core-forming metal if equilibration occurred between the metal and a magma ocean with a bulk silicate Earth composition at an average depth of ~1200 km (~50 GPa and ~3300 K). An O- and Si-enriched buoyant layer may have developed at the top of the outer core as a result of subsequent equilibration with the overlying mantle. **Citation:** Tsuno K., D J. Frost, and D. C. Rubie, (2013), Simultaneous partitioning of silicon and oxygen into the Earth's core during early Earth differentiation, *Geophys. Res. Lett.*, *40*, 66–71, doi: 10.1029/2012GL054116.

1. Introduction

[2] The density of the Earth's outer core is known to be ~10% lower than the density of pure Fe-Ni alloy at the relevant pressure-temperature conditions [e.g., *Anderson and Isaak*, 2002]. This leads to the conclusion that the outer core consists of liquid Fe alloy that contains significant concentrations of one or more light elements. Constraining the light-element budget of the outer core is of fundamental importance for understanding the structure and dynamics of the core and the chemical evolution of the Earth. Light elements that have been identified as potential components of the core include silicon and oxygen [e.g., *Poirier*, 1994]. Arguments for the presence of Si in the core are based on geochemical constraints, such as the superchondritic Mg/Si ratio of the bulk silicate Earth [e.g., *Allègre et al.*, 1995], silicon isotope differences between terrestrial mantle samples and carbonaceous chondrites [e.g., *Georg et al.*, 2007; *Fitoussi et al.*, 2009], and element partitioning during core formation [e.g., *Rubie et al.*, 2011]. Arguments for O being the main light element are based on ab initio calculations and high-pressure experiments. The ab initio calculations of *Alfè et al.*, [2002] indicate that O partitions strongly from the solid inner core into the liquid outer core, and, unlike Si, can explain observed density differences and seismic data. On the other hand, a two-phase ab initio study of metal and silicate liquids has demonstrated that the partitioning of O into the Fe-metal liquid is very limited, at least at 3100 K [*Zhang and Guo*, 2009]. A high-pressure experimental study using inelastic X-ray scattering supports the presence of oxygen in the core [*Badro et al.*, 2007], whereas an X-ray diffraction study [*Sata et al.*, 2010] precludes it. Recent shock experiments also appear to exclude O as the main light element [*Huang et al.*, 2011].

[3] The concentrations of Si and O in the Earth's core must have been established during the early differentiation of the Earth. During formation of the Earth's core, light elements partitioned between silicate melt and segregating liquid metal, probably near the base of magma oceans that formed as a consequence of large high-energy impacts that characterized accretion [e.g., *Rubie et al.*, 2007, 2011]. Therefore, knowledge of the partitioning of Si and O between liquid Fe alloy and silicate melt is necessary to estimate the concentrations of these light elements in the Earth's core. The partitioning of oxygen [*Rubie et al.*, 2004; *Asahara et al.*, 2007; *Frost et al.*, 2010; *Tsuno et al.*, 2011] and silicon [*Wade and Wood*, 2005; *Mann et al.*, 2009] into liquid Fe alloy has been studied separately over a wide range of conditions. However, none of these studies have addressed the possibility that the partitioning of silicon into liquid metal could be influenced significantly by its oxygen concentration and vice versa. Several studies have been performed in which both elements were present in detectable concentrations [*Li and Agee*, 2001; *Takafuji et al.*, 2005; *Kawazoe and Ohtani*, 2006; *Bouhifd and Jephcoat*, 2011; *Ricolleau et al.*, 2011; *Siebert et al.*, 2012]. However, in several of these studies [*Li and Agee*, 2001; *Kawazoe and Ohtani*, 2006; *Ricolleau et al.*, 2011] the mutual concentrations of Si and O were low (e.g., <1 wt %) due to relatively low temperatures. In the study of *Takafuji et al.*, [2005], only silicate perovskite coexisted

---

All Supporting Information may be found in the online version of this article.

[1] Bayerisches Geoinstitut, Universität Bayreuth, D-95440, Bayreuth, Germany.

[2] Department of Earth Science, Rice University, Houston, Texas, 77005, USA.

Corresponding author: Kyusei Tsuno, Department of Earth Science, Rice University, Houston, TX 77005, USA. (Kyusei.Tsuno@rice.edu)

0094-8276/13/2012GL054116

with liquid metal, which makes it difficult to determine oxygen fugacity, which is a critically important controlling parameter. Previous partitioning studies in the diamond anvil cell have generally focused on collecting data as a function of pressure and temperature, whereas data collected as a function of oxygen fugacity at a single pressure and temperature are required for deriving a robust model for the combined partitioning of O and Si.

[4] To investigate the simultaneous partitioning of Si and O between silicate melt and liquid Fe alloy and possible thermodynamic interactions between these elements in liquid Fe, temperatures of a least 3000 K are required to obtain concentrations of >1 wt %. Such temperatures are at the limit of what is currently obtainable with the multianvil apparatus but are potentially at the lower end of the temperature range over which core formation occurred [*Rubie et al.*, 2011]. Here we present new experimental results describing Si and O partitioning between liquid Fe and silicate melt at 25 GPa and up to 3080 K using a multianvil apparatus. A new thermodynamic model is derived from the data that provides an insight into the concentrations of these elements in Earth's core.

2. Experimental Technique

[5] High-pressure experiments were performed using a 1000 tonne Kawai-type multianvil apparatus at 25 GPa and over the temperature range 2770–3080 K. The starting materials were mixtures of pure Fe metal, $MgSiO_3$ glass, SiO_2 powder, and wüstite obtained by the reduction of hematite in a gas-mixing furnace (see Table 1 for compositions). The starting materials were loaded into single crystal MgO capsules, rather than semi-sintered polycrystalline MgO capsules, to minimize the reaction between silicate melt and the capsule wall. The sample assembly consisted of a Cr-doped MgO octahedron with edge lengths of 10 mm, and the corresponding truncation edge lengths of the WC-anvils were 4 mm. Pressure was calibrated as described by *Keppler and Frost* [2005]. The cylindrical heater consisted of $LaCrO_3$ but the customary ZrO_2 insulating sleeve around the heater was dispensed with in order to avoid reaction between $LaCrO_3$ and ZrO_2 that occurs at high temperatures. To also avoid chemical reaction at high temperatures, thermocouples were not used and instead temperatures were estimated from a power-temperature relationship. The latter was calibrated up to ~3100 K in separate experiments, using W3%Re–W25%Re (Type D) thermocouples giving T (K) = 912.75 + 2.858 × W (Watt) between 2700–3100 K and 25 GPa, with a reproducibility of ±5%. The recovered samples were analyzed using a scanning electron microscope (LEO 1530) for textural observations, and an electron microprobe (JEOL JXA-8200) for chemical analysis. The microprobe was operated at a 15 kV accelerating voltage, 15 nA beam current and counting times of 20 s. Standards used for analyzing metal were periclase for O, pure iron for Fe, andradite for Si, enstatite for Mg and for analyzing quenched silicate melt, fayalite was used for Fe and enstatite for Si and Mg. When analyzing oxygen, we found the relative intensity of the O Kα peak to be strongest at 15 kV using a LDE1 spectroscopy crystal. The peak count was found to remain constant over periods of 30 s. We observed no O peak shift between the periclase (standard) and the O-bearing Fe-alloy (sample).

3. Results

[6] The experimental conditions and the chemical compositions of coexisting quenched liquid Fe alloy and silicate melt are summarized in Table 1. The resulting phase assemblages at high *P-T* consisted of liquid Fe alloy + silicate liquid + ferropericlase (Supporting Information, Figure S1). The metal typically segregates to form one large semi-spherical pool and numerous smaller pools (Supporting Information, Figure S1a). The quench texture of silicate liquid was similar in all experiments (Supporting Information, Figure S1b). Two types of quench textures were observed in the metal phase. At relatively lower temperatures (<3000 K), ~5 µm-diameter Fe-Si-O blobs exsolved from the metal during the quench (Supporting Information, Figures S1c and S1d), as described previously [*O'Neill et al.*, 1998; *Gessmann and Rubie*, 1998]. Note that the blobs in the quenched liquid metal cannot be material entrained from the surrounding silicate melt because their magnesium concentrations are essentially zero (based on electron microprobe analyses using a focused beam; see Table S1 in the Supporting Information). Also, the blobs did not originate as a coexisting immiscible oxide-rich liquid at the experimental conditions because, in this case, textures would be quite different [e.g., Figure 9 of *Frost et al.*, 2010]. At temperatures >3000 K, the exsolved oxide phase is present as needle-like Fe-Si-O dendrites ~10 µm long (Supporting Information,Figures S1e and S1f). The large metal pools typically display a rim that is free of blobs or dendrites (Supporting Information, Figures S1c and S1e) because the exsolved Fe-Si-O component re-equilibrates with the silicate liquid during quenching [*O'Neill et al.*, 1998]. The smaller

Table 1. Experimental Conditions and Chemical Compositions of Liquid Fe Alloy and Silicate Liquid at 25 GPa

Run No.[a]	Temp.[b] (K)	Duration (min)	Starting Compositions[c]	Liquid Fe Alloy (wt %)[d]			Silicate Liquid (wt %)[d]		
				Fe	Si	O	SiO_2	FeO	MgO
H2870	2770(140)	3	$MgSiO_3$(60), Fe(40)	97.1(4)	4.0(2)	0.17(3)	53.8(15)	4.4(8)	40.0(9)
H2875	2913(150)	3	$MgSiO_3$(60), $Fe_{98}O_2$(40)	96.7(3)	2.9(1)	0.40(4)	46.3(11)	5.3(8)	46.1(14)
H2881	2913(150)	3	$MgSiO_3$(60), Fe(40)	96.7(5)	2.9(1)	0.41(4)	46.3(11)	5.3(8)	46.1(12)
H2940	2913(150)	3	$(Mg_{0.9}Fe_{0.1}),SiO_3$(20), $Fe_{96}O_4$(80)	96.7(2)	0.56(11)	4.7(5)	41.5(11)	25.1(18)	31.2(14)
H2949	2913(150)	2	$(Mg_{0.8}Fe_{0.2}),SiO_3$(30), $Fe_{96}O_4$(70)	95.8(2)	1.4(1)	2.8(3)	42.9(14)	19.8(25)	34.9(16)
H2956	3056(150)	2	$MgSiO_3$(30), Fe(70)	96.5(6)	3.0(4)	1.1(3)	52.1(26)	8.1(8)	40.3(28)
H2968	3080(150)	2	$(Mg_{0.8}Fe_{0.2}),SiO_3$(30), $Fe_{96}O_4$(70)	96.0(4)	1.3(3)	2.3(4)	50.1(24)	12.6(13)	37.7(21)

[a] All experiments were performed using a split-sphere Kawai-type multianvil apparatus installed at the Bayeriches Geoinstitut.

[b] Temperatures at 25 GPa were calibrated in separate experiments using a type D thermocouple, which is determined to be T (K) = 912.75 + 2.858 × W (Watt) between 2700–3100 K. The temperature errors are shown in parentheses.

[c] The numbers in parentheses show the weight % proportions of silicate and metallic components.

[d] The numerals in parentheses are one standard deviation in terms of the last digits.

metal pools (Figure S1a) often have very low concentrations of Si and O because of extensive re-equilibration with silicate melt during quenching. For this reason only the larger Fe-liquid pools were analyzed for light elements.

[7] Concentrations of Si and O in the liquid metal were determined by performing image analysis and integrating the compositions of metal matrix and exsolved blobs when the blobs were sufficiently large (H2940) [*O'Neill et al.*, 1998]. For the other samples, the quenched metal was analyzed using a defocused electron beam (20 or 50 μm diameter). Measured solubilities range up to ~4 wt % for Si and ~5 wt % for O (Table 1).

[8] The partitioning of Si between silicate and metallic liquids can be described by the equilibrium

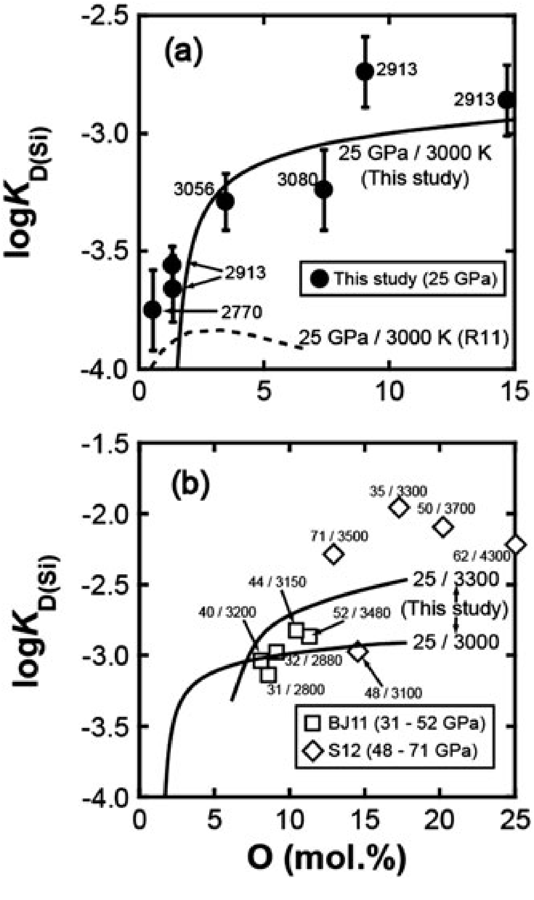

Figure 1. (a) Experimental results at 25 GPa (filled circles) showing the partitioning of Si between liquid Fe metal and silicate melt expressed as $\log K_{D(Si)}$ and plotted as a function of the mol % O content of the metal. Error bars for $\log K_{D(Si)}$ are based on the 1σ standard deviation of the electron microprobe analyses. Each data point is labeled with the experimental temperature in K. The solid line shows the thermodynamic model calculated using equations (3) and (5) at 25 GPa and 3000 K. The dashed line shows the thermodynamic model of *Ricolleau et al.* [2011] calculated at 25 GPa/3000 K over the same range of melt FeO contents as the experiments and the solid curve. (b) The thermodynamic model calculated at 25 GPa and 3000 and 3300 K is compared with the laser-heated diamond anvil cell results of *Siebert et al.* [2012] (S12, open diamonds) and *Bouhifd and Jephcoat* [2011] (BJ11, open squares). Each individual data point is labeled with the experimental pressure and temperature (*P/T*) in GPa and K.

$$\mathrm{SiO_2}^{silicate} + 2\mathrm{Fe}^{metal} = \mathrm{Si}^{metal} + 2\mathrm{FeO}^{silicate} \tag{1}$$

from which a Si distribution coefficient, $K_{D(Si)}$, can be defined, which should be nominally independent of oxygen fugacity (f_{O_2})

$$K_{D(\mathrm{Si})} = \frac{x_{Si}^{metal}\left(x_{FeO}^{silicate}\right)^2}{x_{SiO_2}^{silicate}\left(x_{Fe}^{metal}\right)^2} \tag{2}$$

[9] Here x_{Si}^{met} is, for example, the mole fraction of Si in the metallic liquid. Figure 1 shows $\log K_{D(Si)}$ plotted as a function of the O content of the liquid metal at 25 GPa and 2770–3080 K. Although the Si content of the metal decreases with increasing O content (see Table 1), as expected [Figure 10 of *O'Neill et al.*, 1998], $\log K_{D(Si)}$ actually increases with increasing O content of the metal (Figure 1). Note that increasing O in the metal is equivalent to an increase in both $\log f_{O_2}$ and the silicate FeO content. However, experiments performed at relatively low temperatures, where very little O partitions into the metal, have shown that $\log K_{D(Si)}$ is independent of these two parameters [*Mann et al.*, 2009; *Ricolleau et al.*, 2011]. As the temperatures in all our experiments (with the exception of H2870) are similar, the results indicate that $K_{D(Si)}$ is dependent on the O content of the metal, i.e., the presence of O in liquid metal increases the Si content at a given constant f_{O_2}.

4. Discussion

[10] In order to understand the behavior and interaction of Si and O during core formation, a thermodynamic model is required that describes the partitioning of both elements as a function of either oxygen fugacity or the FeO content of the silicate melt. Two equations describing the partitioning of each element must be solved simultaneously in order to determine the concentration of each element in the metal. The most meaningful approach is to use equations which are internally consistent with each other, with activity-composition expressions that satisfy the Gibbs-Duhem equation. The Si equilibrium constant, K(Si), can be defined in terms of the distribution coefficient $K_{D(Si)}$ and the activity coefficients (γ) of the components in the silicate and metallic phases

$$\log K(\mathrm{Si}) = \log K_{D(\mathrm{Si})} + \log\frac{\gamma_{Si}^{metal}}{\left(\gamma_{Fe}^{metal}\right)^2} + \log\frac{\left(\gamma_{FeO}^{silicate}\right)^2}{\gamma_{SiO_2}^{silicate}} \tag{3}$$

[11] Oxygen partitioning is described through the equilibrium

$$\mathrm{FeO}^{silicate} = \mathrm{Fe}^{metal} + O^{metal} \tag{4}$$

for which the oxygen equilibrium constant, K(O), is defined by

$$\log K(O) = \log\frac{x_{Fe}^{metal}x_{Fe}^{metal}}{x_{FeO}^{silicate}} + \log\frac{\gamma_{Fe}^{metal}\gamma_{O}^{metal}}{\gamma_{FeO}^{silicate}} \tag{5}$$

[12] Silicate melt activity coefficients in both equations (3) and (5) are considered to be unity as they cannot be determined independently with any accuracy at the conditions of the experiments. The activity coefficients (γ) for Fe, Si, and O in a ternary metallic alloy are expressed using the modified Wagner equations of *Ma* [2001], as has become standard practice

$$\begin{aligned}\ln\gamma_{Fe}^{met} &= \varepsilon_O^O(x_O+\ln(1-x_O))+\varepsilon_{Si}^{Si}(x_{Si}+\ln(1-x_{Si}))\\ &+\varepsilon_{Si}^{O}x_Ox_{Si}\left(1-\frac{1}{1-x_O}-\frac{1}{1-x_{Si}}\right)\\ &-\frac{\varepsilon_{\mathrm{Si}}^{O}x_O^2x_{\mathrm{Si}}^2}{2}\left(\frac{3}{1-x_O}+\frac{3}{1-x_{Si}}+\frac{x_O}{(1\text{-}x_O)^2}+\frac{x_{Si}}{(1\text{-}x_{Si})^2}-3\right)\end{aligned} \tag{6}$$

and for O and Si,

$$\begin{aligned}\ln\gamma_i^{met} &= \ln\gamma_{Fe}^{met}+\ln\gamma_i^0-\varepsilon_i^i\ln(1-x_i)\\ &-\varepsilon_{Si}^{O}x_j\left(1+\frac{\ln(1-x_j)}{x_j}-\frac{1}{1-x_i}\right)\\ &+\varepsilon_{Si}^{O}x_j{}^2x_i\left(\frac{1}{1-x_j}+\frac{1}{1-x_i}+\frac{x_i}{2(1-x_i)^2}-1\right)\end{aligned} \tag{7}$$

where x_i is the mole fraction of component i in liquid Fe and j signifies O when i is Si and vice versa. Activity coefficients at infinite dilution in liquid Fe alloy are designated by γ_i^0 and ε_O^O,ε_{Si}^{Si} and ε_{Si}^{O} are interaction parameters describing O-O, Si-Si and Si-O interactions in the Fe liquid. Interaction parameters are reported at a standard temperature of 1873 K, as is the general convention in the Steelmaking Data Sourcebook [*Steelmaking*, 1988] from which $\varepsilon_{Si}^{Si}=12.4$ is taken. The values are extrapolated to higher temperatures using the expression

$$\varepsilon_i^j(T)=\frac{1873}{T}\varepsilon_i^j(1873) \tag{8}$$

[13] The value $\varepsilon_O^O=-1.0$ was refined from the data of *Asahara et al.* [2007] and the model of *Frost et al.* [2010]. The value $\varepsilon_{Si}^{O}=-5.0$ is refined from the current experimental data. Activity coefficients at infinite dilution, $\ln\gamma_{Si}^0=-5.4$ and $\ln\gamma_O^0 = 4.29–16{,}500/T$, are taken also from the Steelmaking Data Sourcebook. An expression describing the equilibrium constant for oxygen, $\log K(\mathrm{O}) = 4.4–15{,}900/T + 1.07P/T$, was derived from the data of *Asahara et al.* [2007] and the model of *Frost et al.* [2010], with P in GPa and T in K. The silicon equilibrium constant is formulated at 25 GPa using the expression $\log K(\mathrm{Si}) = –16{,}800/T$, which was refined from the data of this study.

[14] The curve determined from the simultaneous solution of equations (3) and (5) using the parameters described above and calculated at 3000 K is shown in Figure 1. The calculation is made for melt FeO contents of a similar range to those of the experimental data. As can be seen the model provides a good fit to the O contents of the liquid alloy and $K_{\mathrm{D(Si)}}$ over the experimental range of melt FeO contents, particularly when considering experimental temperature uncertainties of ~150 K. The model also reproduces the apparent effect of O on $K_{D\mathrm{(Si)}}$ over the range of melt FeO contents. The recent model of *Ricolleau et al.* [2011] is also shown in Figure 1a calculated, for comparison, at the same conditions and melt FeO concentration range. This model is in poor agreement with our data and reproduces poorly both the absolute O content of the metal for a given melt FeO content and the relationship between O and Si concentrations. This is because the model does not take suitable account of the interactions between O and Si, most likely as a result of the low mutual concentrations of O (0–1 wt %) and Si (0–1.6 wt %) in the experiments of *Ricolleau et al.*, [2011]. In addition, the concentrations determined at 1 atmosphere that were used to derive data published in the Steelmaking Data Sourcebook, used by *Ricolleau et al.* [2011], were far lower than the concentrations at which O and Si interactions should be detectable.

[15] Liquid metal - liquid silicate partitioning data for O and Si obtained from laser-heated diamond anvil cell experiments at 35–71 GPa and 3100–4300 K [*Siebert et al.*, 2012] are shown in Figure 2b. Diamond anvil cell data obtained at 24.5–28.9 GPa and 2500–2800 K [*Bouhifd and Jephcoat*, 2011] are also shown, although it has been suggested that their sample analyses may be in error [*Wade and Wood*, 2012]. Our model calculations at 25 GPa and 3000 and 3300 K compare well with the results of both these diamond anvil cell studies (Figure 2b), especially considering the likely experimental temperature uncertainties of >100 K. In addition there is no systematic deviation between the model and the data of *Siebert et al.* [2012] implying agreement within the experimental uncertainties. We note that the *Siebert et al.* [2012] data point at 4300 K and 62 GPa is seemingly inconsistent with the rest of the data and with the trend predicted by the model and one data point at 4400 K and 74 GPa has been excluded because it falls far outside of the O range over which the model has been calibrated. Given the generally good agreement between the model at 25 GPa and the available high-pressure experimental data, at least to 71 GPa, we conclude that the effect of pressure on O and Si partitioning is small and is minor in comparison with the effect of temperature.

[16] We have calculated the combined Si and O contents of liquid Fe metal in equilibrium with a peridotitic silicate liquid with a range of FeO contents and $X_{\mathrm{SiO2}} = 0.38$ using the above thermodynamic model at 25 GPa and temperatures from 2750 to 3500 K (Figure 2). The model shows that Si and O are almost mutually exclusive in liquid Fe metal at 25 GPa and temperatures <3000 K, as is the case at 1 bar [Figure 10 of *O'Neill*

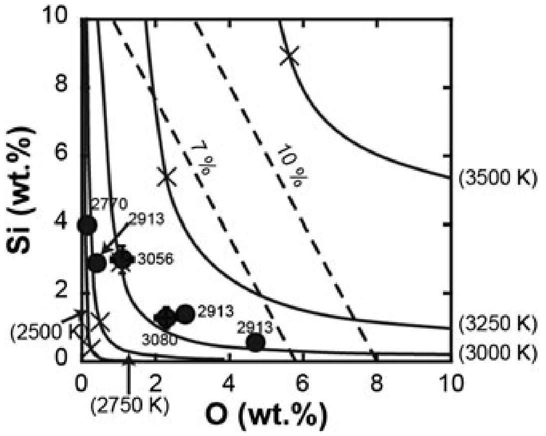

Figure 2. Si and O concentrations in liquid Fe equilibrated with silicate liquid. The experimental data of this study (25 GPa) are plotted as filled circles, each of which is labeled with temperature (K). The solid lines show the thermodynamic model calculated at temperatures from 2500 to 3500 K. Also shown as two dashed lines are the relations between the Si and O contents required to account for 7 and 10% density deficits of Earth's outer core [*Poirier*, 1994]. The crosses on the solid lines show the Si and O contents in metal that is equilibrated with silicate liquid with 8 wt % FeO, i.e., corresponding to the present-day mantle composition.

et al., 1998]. However, as temperature increases to 3000 K, the level at which the Si and O concentrations in the metallic liquid are equal starts to exceed 1 wt %. This equal concentration level increases rapidly with temperature above 3000 K and reaches levels compatible with an outer core density deficit of 7–10% at 3300–3500 K. The equal concentration level is quite close to the concentrations expected for equilibrium with a silicate melt FeO concentration of 8 wt.% (marked by crosses in Figure 2), i.e., that of the present day mantle. This implies that the core's density deficit could be caused by significant concentrations of both Si and O if the average metal-silicate equilibration temperature exceeded 3300 K. Assuming that metal-silicate equilibration occurred close to the peridotite liquidus and that pressure has a negligible effect on partitioning (as discussed above), the minimum average equilibration pressure would then be 45–55 GPa [*Andrault et al*., 2011; *Liebske and Frost*, 2012]. On the other hand, if metal-silicate equilibration during core formation occurred at relatively low pressures and temperatures, e.g., 22.5 GPa and 2673 K [*Righter et al*., 2010], mutual concentrations of both Si and O in the core would both be ~0.2 wt %.

[17] Assuming that pressure has little effect on the mutual partitioning of O and Si, as implied by the available high-pressure data, our thermodynamic model can be used to examine plausible present-day core-mantle interactions. Estimates for the outermost core temperature are generally in the range 3500–4500 K [*Boehler*, 1992, 1993; *Zerr et al*., 1998; *Alfè et al*., 2002; *van der Hilst et al*., 2007]. If the outer core is in equilibrium with a silicate mantle of typical FeO content (~8 wt %) then at these temperatures the outer core would dissolve much more Si and O than the estimated 10 % density deficit would imply (Figure 2). This might have led to the early development of a Si- and O-enriched low-density layer at the top of the outer core [*Buffett and Seagle*, 2010]. As the outer core cools and the equilibrium light-element contents of this layer decrease, the base of the mantle would then become enriched in FeO and SiO_2 that are released from this outer layer.

[18] **Acknowledgments**. We thank Y. Nakajima for assistance and discussions and two anonymous reviewers for helpful comments. This study was funded partly by the German Science Foundation Priority Programmes SPP1115 "Mars and the Terrestrial Planets" (Ru 437/8) and SPP1385 "The first 10 Million Years of the Solar System – a planetary materials approach" (Ru1323/2), the Visiting Scientist Program of the Bayerisches Geoinstitut and the European Research Council (ERC) Advanced Grant "ACCRETE" (contract 290568 to DCR).

References

Alfè, D., M. J. Gillan, and G. D. Price (2002). Composition and temperature of the Earth's core constrained by combining ab initio calculations and seismic data. *Earth Planet. Sci. Lett.*, *195*(1-2), 91–98.

Allègre, C. J., J-. P. Poirier, E. Humler, and A. W. Hofmann (1995). The chemical composition of the Earth, *Earth Planet. Sci. Lett.*, *134*(3-4), 515–526.

Anderson, O. L., and D. G. Isaak (2002), Another look at the core density deficit of Earth's outer core, *Phys. Earth Planet. Inter.*, *131*(1), 19–27.

Andrault, D., N. Bolfan-Casanova, G. Lo Nigro, A. Bouhifd, G. Garbarino, M. Mezouar (2011), Solidus and liquidus profiles of chondritic mantle: Implication for melting of the Earth across its history. *Earth Planet. Sci. Lett.*, *304*, 251–259.

Asahara, Y., D. J. Frost, and D. C. Rubie (2007), Partitioning of FeO between magnesiowüstite and liquid iron at high pressures and temperatures: Implications for the composition of the Earth's outer core, *Earth Planet. Sci. Lett.*, *257*(3-4), 435–449.

Badro, J., G. Fiquet, F. Guyot, E. Gregoryanz, F. Occelli, D. Antonangeli, and M. d'Astuto 259 (2007), Effect of light elements on the sound velocities in solid iron: Implications for the composition of Earth's core, *Earth Planet. Sci. Lett.*, *254*(1-2), 233–238.

Boehler, R. (1992), Melting of the Fe-FeO and the Fe-FeS systems at high pressure: Constraints on core temperatures, *Earth Planet. Sci. Lett.*, *111*, 217–227.

Boehler, R. (1993), Temperatures in the Earth's core from melting point measurements of iron at high static pressures, *Nature*, *363*, 534–536.

Bouhifd, M. A., and A. P. Jephcoat (2011), Convergence of Ni and Co metal-silicate partition coefficients in the deep magma-ocean and coupled silicon-oxygen solubility in iron melts at high pressures, *Earth Planet. Sci. Lett.*, *307*(3-4), 341–348.

Buffett, B. A., and C. T. Seagle (2010), Stratification of the top of the core due to chemical interactions with the mantle, *J. Geophys. Res.*, *115*, B04407, doi:10.1029/2009JB006751.

Fitoussi, C., B. Bourdon, T. Kleine, F. Oberli, and B. C. Reynolds (2009), Si isotope systematics of meteorites and terrestrial peridotites: implications for Mg/Si fractionation in the solar nebula and for Si in the Earth's core, *Earth Planet. Sci. Lett.*, *287*(1-2), 77–85.

Frost, D. J., Y. Asahara, D. C. Rubie, N. Miyajima, L. S. Dubrovinsky, C. Holzapfel, E. Ohtani, M. Miyahara, and T. Sakai (2010), Partitioning of oxygen between the Earth's mantle and core, *J. Geophys. Res.*, *115* (B2), B02202. doi:10.1029/2009JB006302.

Georg, R. B., A. N. Halliday, E. A. Schauble, and B. C. Reynolds (2007), Silicon in the Earth's core, *Nature*, *447*(7148), 1102–1106.

Gessmann, C.K., and D. C. Rubie (1998), The effect of temperature on the partitioning of Ni, Co, Mn, Cr and V at 9 GPa and constraints on formation of the Earth's core. *Geochim. Cosmochim. Acta*, *62*, 867-882.

Huang, H., Y. Fei, L. Cai, F. Jing, X. Hu, X. Xie, L. Zhang, and Z. Gong (2011), Evidence for an oxygen-depleted liquid outer core of the Earth, *Nature*, *479*, 513–516.

Japan Society For The Promotion Of Science (1988), *Steelmaking Data Sourcebook*, Gordon and Breach, New York.

Kawazoe, T., and E. Ohtani (2006), Reaction between liquid iron and (Mg,Fe)SiO_3-perovskite and solubilities of Si and O in molten iron at 27 GPa, *Phys. Chem. Miner.*, *33*, 227–234.

Keppler, H., and D. J. Frost (2005), Introduction to minerals under extreme conditions. In: R. Miletich, Editor, *Mineral Behaviour at Extreme Conditions, European Mineralogical Union Lecture Notes in Mineralogy vol. 7, EMU*, pp. 1–30.

Li, J., and C. B. Agee (2001), Element partitioning constraints on the light element composition of the Earth's core, *Geophys. Res. Lett.*, *28* (1), 81–84.

Liebske, C., and D.J. Frost (2012), Melting phase relations in the MgO-$MgSiO_3$ system between 16 and 25 GPa: Implications for melting in Earth's deep interior. *Earth Planet. Sci. Lett.*, *345-348*, 159–170.

Ma, Z. T. (2001), Thermodynamic description for concentrated metallic solutions using interaction parameters. *Metallur. Materials Trans. B*, *32*, 87–103.

Mann, U., D. J. Frost, and D. C. Rubie (2009), Evidence for high-pressure core-mantle differentiation from the metal-silicate partitioning of lithophile and weakly-siderophile elements, *Geochim. Cosmochim. Acta*, *73*(24), 7360–7386.

O'Neill, H.St.C., D. Canil, D.C. Rubie, (1998) Metal-oxide equilibria to 2500 °C and 25 GPa: implications for core formation and the light component in the Earth's core. *J. Geophys. Res.*, *103*, 12239–12260.

Poirier, J.-P. (1994), Light elements in the Earth's outer core: A critical review, *Phys. Earth Planet. Inter.*, *85*(3-4), 319–337.

Ricolleau, A., Y. Fei, A. Corgne, J. Siebert, J. Badro (2011) Oxygen and silicon contents of Earth's core from high pressure metal–silicate partitioning experiments, *Earth Planet. Sci. Lett.*, *310*, 409–421.

Righter, K., K.M. Pando, L. Danielson, Cin-Ty Lee (2010) Partitioning of Mo, P and other siderophile elements (Cu, Ga, Sn, Ni, Co, Cr, Mn, V, and W) between metal and silicate melt as a function of temperature and silicate melt composition, *Earth Planet. Sci. Lett.*, *291*, 1–9.

Rubie, D. C., C. K. Gessmann and D. J. Frost (2004) Partitioning of oxygen during core formation on the Earth and Mars. *Nature*, *429*, 58–61.

Rubie, D. C., D. J. Frost, U. Mann, Y. Asahara, F. Nimmo, K. Tsuno, Ph. Kegler, A. Holzheid, and H. Palme (2011), Heterogeneous accretion, composition and core-mantle differentiation of the Earth, *Earth Planet. Sci. Lett.*, *301*(1-2), 31–42.

Rubie, D. C., F. Nimmo, and H. J. Melosh (2007), Formation of the Earth's core. *Treatise on Geophysics*. In: Stevenson, D. (Ed.), *Evolution of the Earth, 9*. Elsevier, Amsterdam, pp. 51–90.

Sata, N, K. Hirose, G. Shen, Y. Nakajima, Y. Ohishi, and N. Hirao (2010), Compression of FeSi, Fe_3C, $Fe_{0.95}O$, and FeS under the core pressures and implication for light element in the Earth's core, *J. Geophys. Res.*, *115*, B09204, doi:10.1029/2009JB006975.

Siebert, J., J. Badro, D. Antonangeli, and F. J. Ryerson (2012), Metal–silicate partitioning of Ni and Co in a deep magma ocean, *Earth Planet. Sci. Lett.*, *321–322*, 189–197.

Takafuji, N., K. Hirose, M. Mitome, and Y. Bando (2005), Solubilities of O and Si in liquid iron in equilibrium with (Mg,Fe)SiO_3 perovskite and the light elements in the core, *Geophy. Res. Lett.*, *32*(6), L06313. doi:10.1029/2005GL022773.

Tsuno, K., D. J. Frost, and D. C. Rubie (2011), The effects of nickel and sulphur on the core–mantle partitioning of oxygen in Earth and Mars, *Phys. Earth Planet. Inter.*, *185*, 1–12.

van der Hilst, R. D., M. V. de Hoop, P. Wang, S.-H. Shim, P. Ma, and L. Tenorio (2007), Seismostratigraphy and thermal structure of Earth's core-mantle boundary region, *Science*, *315*, 1813–1817.

Wade, J., and B. J. Wood (2005), Core formation and the oxidation state of the Earth, *Earth Planet. Sci. Lett.*, *236*(1-2), 78–95.

Wade, J. and B. J. Wood (2012), Metal–silicate partitioning experiments in the diamond anvil cell: A comment on potential analytical errors, *Phys. Earth Planet. Lett.*, *192–193*, 54–58.

Zerr, A., A. Diegeler, and R. Boehler (1998), Solidus of the Earth's deep mantle, *Science*, *281*, 243–245.

Zhang, Y and G. Guo (2009), Partitioning of Si and O between liquid iron and silicate melt: A two-phase ab-initio molecular dynamics study, *Geophys. Res. Lett.*, *36*, L18305.doi:10.1029/2009GL039751.